Applied Catalysis B: Environmental 242 (2019) 194–201

Contents lists available at ScienceDirect

Applied Catalysis B: Environmental

journal homepage: www.elsevier.com/locate/apcatb

Bio-organic–inorganic hybrid photocatalyst, TiO_2 and glucose oxidase composite for enhancing antibacterial performance in aqueous environments

Byoung Chan Kim[a,b,*], Eunhoo Jeong[b,c], Eunju Kim[b,c], Seok Won Hong[b,c]

[a] Center for Environment, Health and Welfare Research, Korea Institute of Science and Technology (KIST), Hwarangno 14-gil 5, Seoul 02792, Republic of Korea
[b] Department of Energy and Environmental Engineering, University of Science and Technology (UST), Hwarangno 14-gil 5, Seongbuk-gu, Seoul 02792, Republic of Korea
[c] Center for Water Resources Cycle Research, Korea Institute of Science and Technology (KIST), Hwarangno 14-gil 5, Seongbuk-gu, Seoul 02792, Republic of Korea

ARTICLE INFO

Keywords:
TiO_2
Glucose oxidase
Hybrid catalyst
Glucose
Antibacterial agent

ABSTRACT

TiO_2-UV photocatalytic systems have been widely studied and applied for removing pathogenic bacteria in water treatment. We created a hybrid catalyst (TiO_2-GOx) by combining the inorganic photocatalyst (TiO_2) and the organic biocatalyst, glucose oxidase (GOx) that can be activated using UV radiation and glucose to generate a reactive oxygen species (ROS). More rapid disinfection of bacteria in the presence of UV and glucose was observed using the hybrid catalyst (TiO_2-GOx) than using TiO_2 particles. GOx generates H_2O_2 and superoxide under glucose-rich conditions in which heterotrophic bacteria grow quickly, this H_2O_2 and superoxide can act as disinfection agents along with the ROS (such as OH radicals) generated from the photocatalytic activation resulting from the interaction between UV radiation and TiO_2. Therefore, the rapid disinfection activity of TiO_2-GOx can be attributed to the enhancement of ROS generation due to the high catalytic activity of TiO_2-GOx in the combined glucose–UV rich environment. The hybrid catalyst (TiO_2-GOx) can be useful for disinfecting field water or wastewater with a high concentration of carbon sources such as glucose that can be assimilated by heterotrophic bacteria.

1. Introduction

UV-assisted TiO_2 inactivation of microorganisms such as pathogenic bacteria has garnered much attention in recent years due to its high efficiency in generating an antibacterial effect in aqueous environments [1–3]. During UV irradiation, highly reactive oxygen species (ROS) such as superoxide radical anions ($^{\cdot}O_2^-$), hydrogen peroxide (H_2O_2), hydroxyl radicals ($^{\cdot}OH$), hydroxyl ions (OH^-), and singlet oxygen ($^1O_2$) are generated [4]; these species are generally considered to be responsible for the inactivation of microorganisms by breaking their outer membranes or disrupting DNA inside cells [1,2]. However, an examination of the literature reveals that there is still disagreement as to which species of reactive oxygen is the major cause for the inactivation of microorganisms: H_2O_2, hydroxyl radicals, or other species [5–7]. Although the controversial issue of the major active ROS has not been resolved, it is known that the lifetime of most ROS created from UV-assisted TiO_2 photocatalytic reactions is very short both in aqueous environments and inside living cells [4,8]. Thus, to achieve the sustainable inactivation of microorganisms, it is important to ensure that ROS, regardless of species, are continuously produced in disinfection applications. H_2O_2 is an ROS that is widely used as a biocide for disinfection in a number of food-related, medical, industrial, and environmental applications, as its decomposition produces non-toxic by-products [9]. The disinfection activity of H_2O_2 is generally believed to result from the formation of highly reactive hydroxyl radicals via the interaction of the superoxide radical anion and H_2O_2 in aqueous environments [10]. Furthermore, it is believed that extremely short-lived hydroxyl radicals within living cells can be catalyzed by the presence of transition metal ions such as Fe^{2+} and H_2O_2 via the “Fenton reaction” [11]. Therefore, regardless of whether hydroxyl radicals or H_2O_2 is the main contributor to the disinfection of bacterial cells, the continuous production of H_2O_2 and other ROS is very important for maintaining the disinfection properties in aqueous environments.

Surface water, groundwater, and drinking water can be contaminated by wastewater effluents containing pharmaceuticals, hormones, chemicals in consumer products, chemicals used in farming, and

* Corresponding author at: Center for Environment, Health and Welfare Research, Korea Institute of Science and Technology (KIST), Hwarangno 14-gil 5, Seoul 02792, Republic of Korea.
E-mail address: bchankim@kist.re.kr (B.C. Kim).

https://doi.org/10.1016/j.apcatb.2018.09.102
Received 3 August 2018; Received in revised form 28 September 2018; Accepted 30 September 2018
Available online 02 October 2018
0926-3373/ © 2018 Elsevier B.V. All rights reserved.

other organic compounds, all of which increase the total organic carbon (TOC) or dissolved organic carbon (DOC) content of field water [12]. Field water with a high TOC or DOC contains large amounts of carbon that can be utilized by heterotrophic bacteria. Among carbon sources, the sugar glucose is the most favorable for the growth of heterotrophic bacteria [13,14]. This leads to the very well-known phenomena of carbon catabolic repression (CCR), in which the presence of glucose prevents the other use of carbon sources for bacterial growth [14]. The oxidation of glucose by glucose oxidase (GOx) resulting in the production of gluconic acid and H_2O_2 is a common reaction in aqueous environments [15,16]. During the production of H_2O_2 in this catalytic reaction, superoxide is also generated as an intermediate through the utilization of dioxygen by GOx [16]. For this reason, GOx with glucose has been used to stabilize food, as it prevents the problems that arise from the presence of oxygen and protects food from microbial growth by producing H_2O_2 [17–21]. In terms of the heterotrophic microorganisms present in field water environments, microorganisms such as bacteria need essential carbon sources such as glucose to grow. Thus, the various ROS such as H_2O_2 or superoxide produced by GOx from the glucose in field water can be used disinfect the environment.

Hence, we hypothesize that the synergetic production of ROS can be triggered by both inorganic (TiO_2) and organic (GOx) catalysts compared to TiO_2 that cannot utilize glucose under UV irradiation in the presence of glucose if both materials exist together as hybrid composites. The antibacterial activity of GOx can be enhanced by combining GOx with TiO_2 particles to facilitate increased production of ROS in aqueous environments containing glucose. The glucose in either field water or wastewater could be utilized by GOx on the surface of TiO_2 in water to produce H_2O_2 or superoxide, which would exhibit antibacterial activity in conjunction with the OH radicals [5] produced by TiO_2 under UV irradiation (Fig. 1). In addition, the reduction in the glucose level in the aqueous environment via the catalytic reaction of glucose with GOx could prevent the growth of microorganisms in an aqueous environment. Therefore, we prepared a TiO_2-GOx inorganic–organic hybrid catalyst and investigated its performance in microorganism removal, using *Escherichia coli* (*E. coli*) as a model bacterium, and compared it to that of TiO_2 particles in the presence of UV radiation and glucose. The quantity and status of GOx immobilized on the surface of TiO_2, the effect of the glucose concentration on disinfection, the synergetic generation of ROS, and the effect of catalase on the synergetic generation of ROS (especially H_2O_2) were examined, and the performance of the hybrid catalyst was compared to that of TiO_2 particles alone.

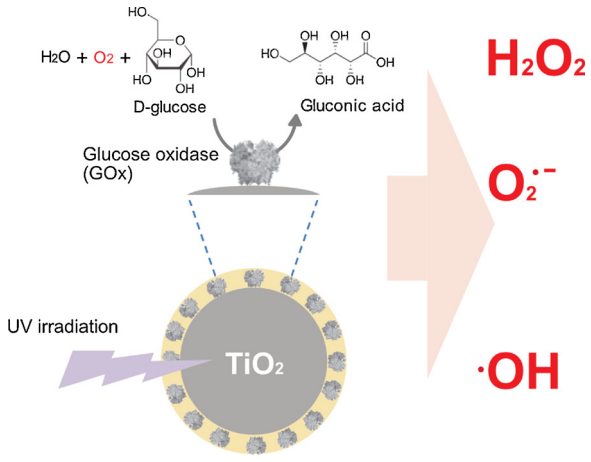

Fig. 1. Schematic of the production of ROS by TiO_2-GOx particles.

2. Materials and methods

2.1. Materials

The TiO_2 particles (P-25) used in this study were purchased from Degussa Evonik GmbH (Germany). GOx, catalase (CAT), D-(+)-glucose, 5,5-Dimethyl-1-pyrroline N-oxide (DMPO), and methylene blue (MB) were purchased from Sigma-Aldrich (St. Louis, MO, USA). Phosphate-buffered saline (PBS) was purchased from Mediatech, Inc. (Manassas, VA, USA). The BCA protein assay kit was purchased from ThermoFisher Scientific (Waltham, MA, USA). *Escherichia coli* (*E. coli*, KCTC2571) and *Bacillus subtilis* (*B. subtilis*, KCTC 1022) were purchased from the Korean Collection for Type Culture (KCTC). Nutrient broth and nutrient agar were purchased from Becton, Dickinson, and Company (Franklin Lakes, NJ, USA).

2.2. Preparation and characterization of TiO_2-GOx hybrid catalysts

TiO_2-GOx was prepared by mixing TiO_2 particles (40.0 mg) with dissolved GOx (0, 0.5, 1.0, 2.5, 5.0, 10.0, and 20.0 mg) in 1 X PBS at varying pH values of 3.0, 5.0, 7.0, and 10.0. The amount of GOx immobilized on the surface of TiO_2 was analyzed using the BCA protein assay kit. After finding an appropriate pH level for the immobilization of GOx on TiO_2 (see Results and Discussion), TiO_2 (40.0 mg) and GOx (20.0 mg) were mixed in a glass vial and sonicated slightly at pH 3.0 to investigate whether there was an antibacterial effect or any photodegradation of MB. The glass vial containing TiO_2 and GOx was incubated at room temperature while being shaken (200 rpm) for 3 h. After incubation at pH 3.0, the mixture was centrifuged (13,500 rpm for 10 min) at 4 °C and the supernatant, which contained the GOx had not been adsorbed onto the TiO_2 surface was removed. The centrifuged particles were suspended in 1 X PBS (pH 7.0) and then centrifuged (13,500 rpm for 10 min) at 4 °C again. The pH of the solvent was changed from 3.0 to 7.0 at this stage because GOx is active through a relatively broad pH range of between 4.0–7.0. This process was repeated thrice. Finally, the particles were suspended in 1 X PBS (pH 7.0) to make a 10.0 mg/mL particle solution, which was then kept at 4 °C until it was used. The surfaces of TiO_2 and TiO_2-GOx were analyzed using an Infinity Gold Fourier transform infrared (FT-IR) spectrometer (ThermoFisher Scientific, MA, USA). The morphology and elemental composition of the particle surfaces were analyzed using a scanning electron microscope (SEM, Teneo VolumeScope, FEI, OR, USA) equipped with energy-dispersive X-ray spectroscopy (EDX, QUAJTA 200 FEG, AMETEK®, PA, USA) and with an acceleration voltage of 15 kV. Raman spectra were carried out on a Raman spectrophotometer (inVia™ Raman microscope, RENISHAW, England) equipped with an Ar laser excitation wavelength of 532 nm. The X-ray photoelectron spectroscopy (XPS) measurements were carried out using an electron spectrometer (PHI 5000 VersaProbe, ULVAC-PHI, Inc., Kanagawa, Japan). The amount of H_2O_2 produced was measured using the Amplex red/horseradish peroxidase reaction (Molecular Probes, Eugene, OR, USA). Electron spin resonance (ESR) spectroscopy (JES-X310, JEOL, Tokyo, Japan) was used to compare the production of reactive oxygen species (ROS) by TiO_2 and TiO_2-GOx in the presence of glucose (5 mg/mL). The spin trap reagent, DMPO was used for trapping $OH^{\cdot}$ radicals and superoxide. Suspension mixtures of 10 mM of DMPO, 5 mg/mL of glucose, and 0.2 mg/mL of TiO_2 or TiO_2-GOx in 1 X PBS (pH 7.0) were prepared. The suspensions were exposed to UV radiation (4-W lamps; spectral maximum: 352 nm; Sankyo Denki; Japan) in a black box for 10 min, followed by immediate ESR measurement.

2.3. Inactivation of bacteria

E. coli (KCTC 2571) was used as a model bacterium to test the inactivation properties of the TiO_2 and TiO_2-GOx particles prepared. The *E. coli* cells were cultivated at 37 °C in a medium containing nutrient

broth until ~1 × 10^7 CFU (colony forming unit)/mL was reached. They were then recovered through centrifugation (4000 rpm for 20 min) at room temperature, washed thrice using 1 X PBS (pH 7.0), and suspended using 1 X PBS (pH 7.0) containing 0, 0.5, 2.5, or 5.0 mg/mL of glucose to prepare an *E. coli* suspension. To investigate the catalase effect, catalase (5 mg/mL) was mixed into the *E. coli* suspension containing glucose (5.0 mg/mL). The *E. coli* suspension (3 mL) was mixed with TiO_2 or TiO_2-GOx particles (0.08 mg/mL) and the resulting suspension was incubated using a 24-well plate set in a shaking incubator (200 rpm) inside a black box. Two 4-W UV lamps (spectral maximum: 352 nm; Sankyo Denki; Japan) were placed inside the black box, which was sealed to prevent light from entering the box. After UV irradiation, 100 µL of the suspension was sampled and diluted with autoclaved water to obtain a moderate cell density. The diluted samples were spread on nutrient agar plates and incubated for ~17 h at 37 °C to determine the number of CFU. *B. subtilis* cells (KCTC 1022) were also cultivated at 37 °C in a medium containing nutrient broth until ~1 × 10^7 CFU/mL was reached for the inactivation test. The number of bacterial colonies was expressed as $\log(N/N_0)$ where N_0 is the CFU/mL at 0 h and N is the CFU/mL at a given times.

2.4. Photodegradation of methylene blue

The photocatalytic activity of the TiO_2 or TiO_2-GOx particles was determined by analyzing the degradation of MB under UV irradiation after adding the particles (2.0 mg) to 35 mL of MB solution (20 µM, pH 6.6) containing 2.0 mg/mL of glucose. The photodegradation test for MB was performed in a quartz vial reactor fitted with two 4-W UV lamps (spectral maximum: 352 nm; Sankyo Denki; Japan) and a magnetic stirrer inside the black box. The reaction mixture was stirred under UV irradiation, after which 1 mL of the mixture was sampled from the quartz vial reactor. The samples were then centrifuged (13,500 rpm for 10 min) to remove the particles from the mixture. The degree of photodegradation of MB was calculated by measuring the absorbance of the residual MB and comparing it to the initial absorbance at 660 nm using a UV–vis spectrophotometer (Shimadzu UV-2550, Japan) after the particles were removed.

3. Results and discussion

3.1. Preparation of TiO_2-GOx hybrid catalyst

We prepared GOx-immobilized TiO_2 particles (TiO_2-GOx) via the adsorption approach, measured the maximum amount of GOx adsorbed on the surface of TiO_2 at different pH levels. The interaction between TiO_2 and proteins has been extensively studied because TiO_2 is widely used in our daily lives, e.g., in paint, bio-medical and implantable materials, cosmetics, and coloring agents for food [22–24]. Many studies have reported that proteins frequently adsorb on TiO_2 [23–25]. Therefore, we used the adsorption approach to immobilize GOx on the surface of TiO_2 particles to prepare the TiO_2-GOx hybrid catalyst without modifying them. Fig. 2 shows the amount of GOx adsorbed onto 40.0 mg of TiO_2 at pH 3.0, 5.0, 7.0, and 10.0. The values of C_{max} (possible maximum amount of GOx on TiO_2) derived from the regression of the adsorption isotherm equation at pH values of 3.0, 5.0, 7.0, and 10.0 were 4.5, 3.3, 2.8, and 2.4 mg, respectively. The C_{max} value decreased with increasing pH up to pH 10.0. Although the exact interaction mechanisms between GOx and TiO_2 are not fully understood, we suspect that the amphiphilic nature of GOx and TiO_2 enables hydrophobic interaction between GOx and TiO_2, and the hydrophilic surface of GOx allows TiO_2-GOx to remain suspended in an aqueous environment [26], unlike TiO_2 (Fig. 3(A)). Therefore, we first prepared TiO_2-GOx at pH 3. Subsequently, the storage and performance tests of the prepared catalysts were carried out at pH 7, because the optimal pH for the GOx reaction is ~4–7 in a buffered solution [27]. The BCA analysis did not reveal the release of GOx from the surface of TiO_2 at pH 7.

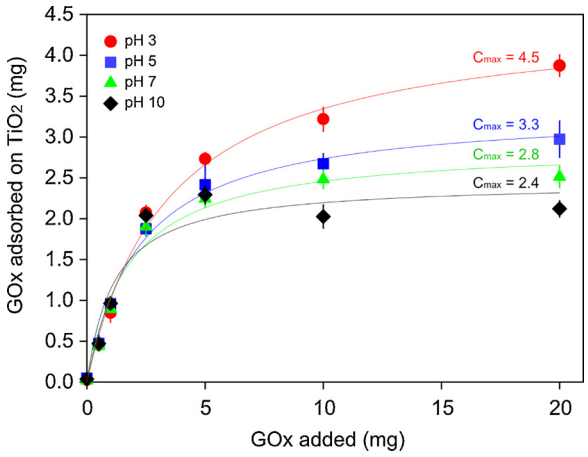

Fig. 2. Absorption of GOx on the surface of TiO_2 at different pH levels.

3.2. Characterization of TiO_2-GOx

We investigated the characteristics of TiO_2-GOx and TiO_2 via FT-IR, SEM-EDX, Raman spectroscopy, and XPS analysis. Fig. 3(B) shows the FT-IR spectra of both TiO_2-GOx and pristine TiO_2 particles. A clear difference in the FT-IR peaks at approximately 1530 cm^{-1} and 1650 cm^{-1} was observed for TiO_2-GOx compared to pristine TiO_2. These peaks correspond to amide I and II from the enzymes (proteins). The amide I peak at ~1650 cm^{-1} is due to the C═O stretching vibration of the peptide bonds of the enzyme. In contrast, the amide II peak at ~1530 cm^{-1} is due to in-plane NH bending and the CN stretching vibration [28,29]. These two peaks provide substantial evidence for the presence of GOx on the surface of the TiO_2 particles. Therefore, we concluded that the TiO_2-GOx particles were successfully fabricated. The image in Fig. 3(A) shows the precipitation of the pristine TiO_2 particles and the suspension of TiO_2-GOx in 1 X PBS buffer (pH 7.0) after 5 min of mixing. The pristine TiO_2 underwent a significant amount of precipitation in the PBS buffer, but a yellowish suspension was observed for TiO_2-GOx. As described above, it was hypothesized that the amphiphilic surface of the GOx adsorbed onto the TiO_2 particles made the TiO_2 hydrophilic [26]. This is more evidence of the successful adsorption of GOx onto the surface of the TiO_2 particles.

Fig. 4 shows the SEM images of TiO_2 and TiO_2-GOx along with the corresponding EDS analyses. The morphology of TiO_2 (Fig. 4(A)) and TiO_2-GOx (Fig. 4(B)) was almost the same in the SEM images. The adsorbed GOx did not significantly alter the surface morphology of the TiO_2. Because the molecular size of GOx (less than 10 nm) [30] was smaller than that of TiO_2, the structure of GOx could not be clearly observed on the TiO_2 surface through SEM. However, the EDX of the TiO_2-GOx particles demonstrated the presence of the element carbon from GOx, which was not observed for the pristine TiO_2 particles. The EDX results indicated that the TiO_2-GOx contained 4.21 wt% C and 9.26 at% C.

Fig. 5 shows the Raman spectra of TiO_2 and TiO_2-GOx. Most notably, no differences were observed between the Raman peaks of TiO_2-GOx and those of pristine TiO_2. Some peaks (397, 514, and 639 cm^{-1}) that have been previously reported for commercial P25 TiO_2 were observed in both TiO_2 and TiO_2-GOx [31–33]. This indicated that the chemical composition and structure of the pristine TiO_2 particles were not changed when the enzyme (GOx) was attached to the surface of the particles. Normally, proteins show significant peaks between 800 and 1500 cm^{-1} in Raman spectra [34]. Therefore, we expected that such peaks would be observed in the TiO_2-GOx spectrum between 800 and 1500 cm^{-1}. However, only some additional noise compared to the pristine TiO_2 particle spectrum was observed. This was probably

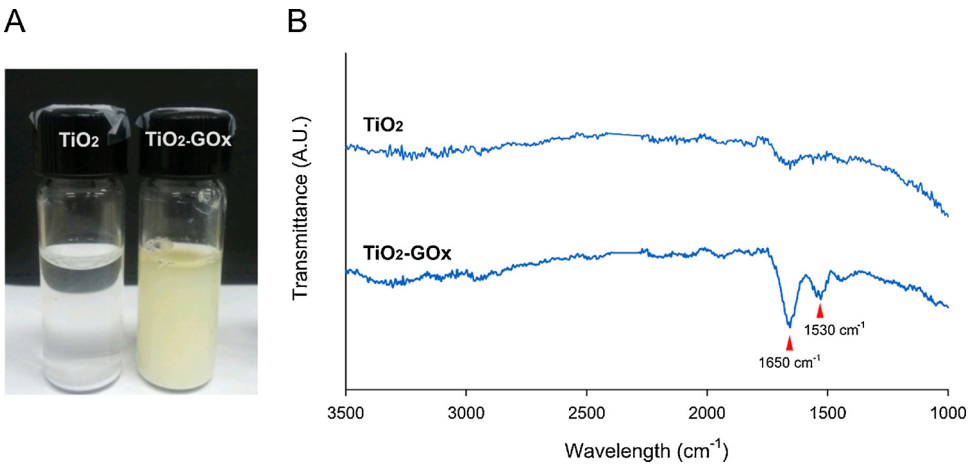

Fig. 3. (A) An image of the suspensions of TiO_2 and TiO_2-GOx. (B) FT-IR spectra of TiO_2 and TiO_2-GOx.

because the amount of GOx attached was relatively small compared to the total amount of TiO_2 particles.

The surface chemical composition of TiO_2 and TiO_2-GOx was investigated using XPS, and the results are shown in Fig. 6. The overall XPS survey curve in Fig. 6(A) shows that Ti and O were the main components of TiO_2, while N was observed only for TiO_2-GOx. The Ti composition did not change after the immobilization of GOx (Fig. 6(B)). The N observed for TiO_2-GOx was attributed to the composition of the protein GOx, which was not present on the pristine TiO_2. The strong peak observed near 400 eV indicated that the sample contained amine ($-NH_2$) from proteins [35]; the enzymatic protein, GOx, has many amine groups (Fig. 6(C)). The O1 s spectrum of TiO_2-GOx in Fig. 6(D) demonstrates the presence of another type of chemical group with a binding energy of 532.4 eV (peak 3) that did not occur in pristine TiO_2. Peak 1 (529.7 eV) and peak 2 (531.0 eV) are usually observed for TiO_2 particles while peak 3 (532.4 eV) has been reported for proteins [35]. The combined results of the FT-IR, SEM with EDX, and Raman spectra, and XPS analysis showed that GOx was attached well on the surface of TiO_2 without seriously altering the structure of TiO_2.

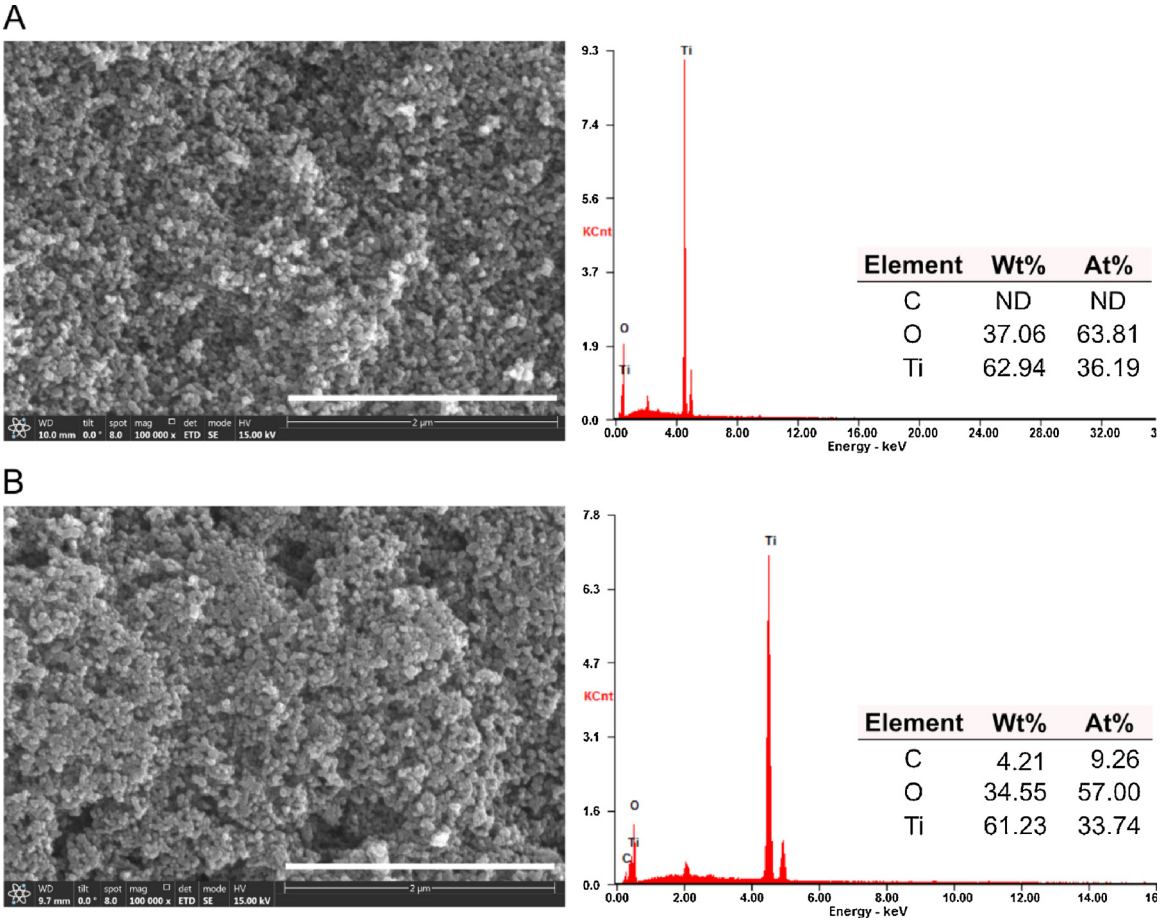

Fig. 4. SEM images and EDS analysis of (A) TiO_2 and (B) TiO_2-GOx (White bars in the SEM images indicate 2 μm).

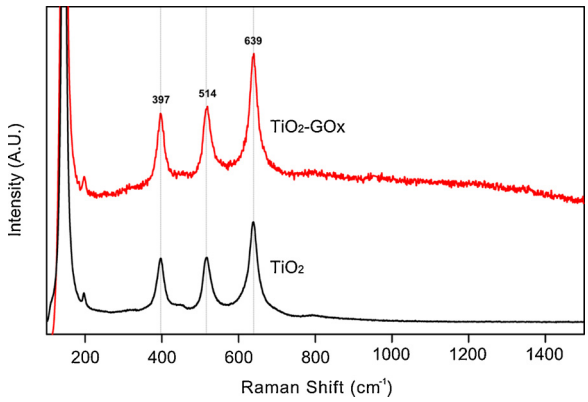

Fig. 5. Raman spectra of TiO_2 and TiO_2-GOx.

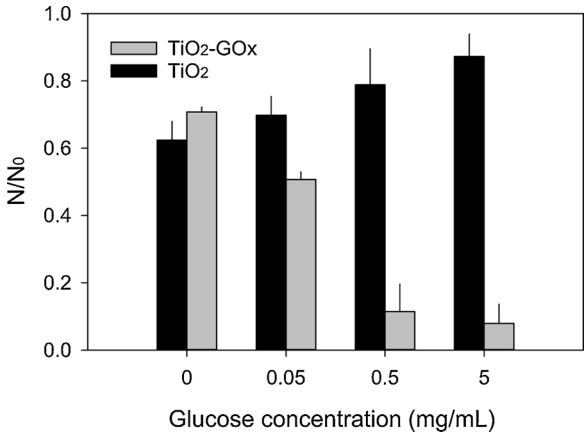

Fig. 7. Comparison of the antibacterial performance of TiO_2 and TiO_2-GOx at different glucose concentrations.

3.3. Catalytic performance of TiO_2-GOx

We tested the antibacterial performance of TiO_2-GOx and TiO_2 15 min after UV exposure in the presence of different glucose concentrations using *E. coli* as a model bacterium. Fig. 7 shows the effect of the glucose concentration on the inactivation of *E. coli* by pristine TiO_2 and TiO_2-GOx. The antibacterial performance of pristine TiO_2 decreased with increasing glucose concentration, while that of TiO_2-GOx increased. The antibacterial performance of TiO_2 in the presence of 5.0 mg/mL of glucose was very poor, while that of TiO_2-GOx was the highest at this concentration. These results suggest that in samples containing a high amount of glucose, the TiO_2-UV assisted antibacterial process may not be effective in killing microorganisms. It also appears that bacterial cells have a tolerance the ROS generated via the TiO_2-UV reaction at a high concentration of glucose, which is the most favorable carbon source for the growth of bacteria. However, in the presence of TiO_2-GOx, glucose acts as an ROS generator (H_2O_2) rather than a source for growth. Then, we compared the antibacterial performance of TiO_2-GOx and TiO_2 with glucose (5.0 mg/mL) and without glucose under UV exposure over time using *E. coli* as the model bacterium. The $\log(N/N_0)$ values, which indicate the antibacterial activity of TiO_2 (no glucose), TiO_2-GOx (no glucose), TiO_2 (5 mg/mL glucose), and TiO_2-GOx (5 mg/mL glucose) after 45 min under UV exposure, were −1.03, −0.49, −0.33, and −1.98, respectively (Fig. 8(A)), although antibacterial activity was observed in all the cases. The improved antibacterial activity of TiO_2-GOx in the presence of glucose can be explained by the synergetic production of ROS generated from TiO_2 activation via UV exposure and glucose oxidation by the glucose oxidase on the surface of TiO_2 (Fig. 1). The inactivation activity of TiO_2-GOx for *E. coli* in the presence of glucose was excellent compared to that of pristine TiO_2. The

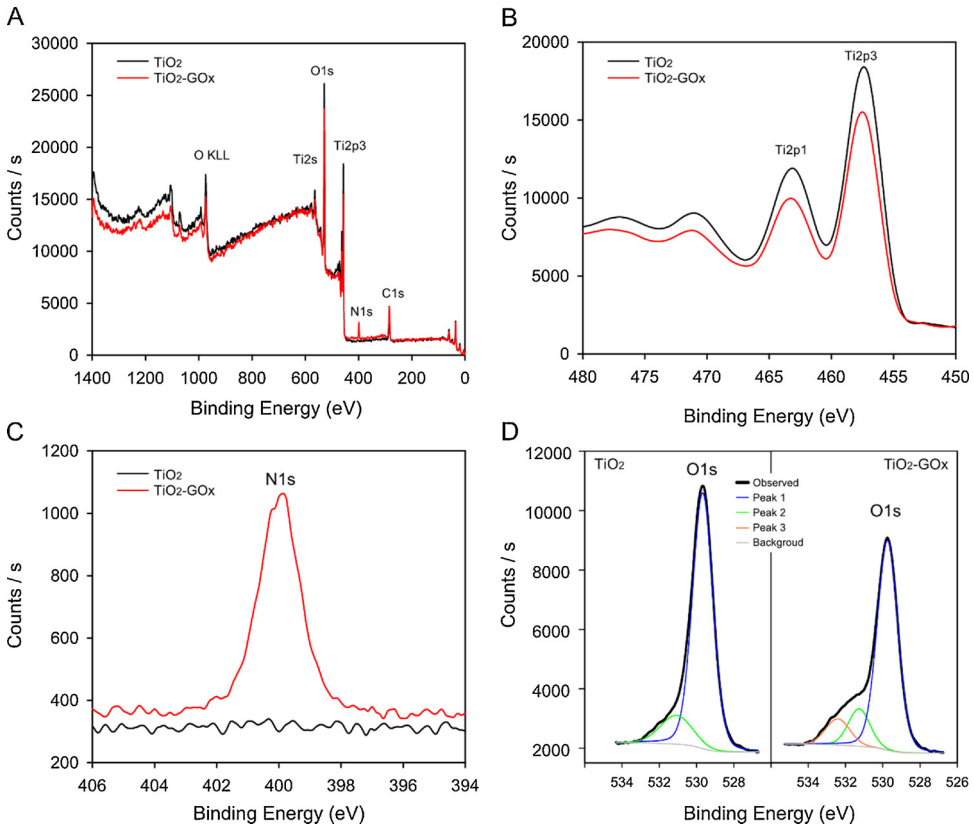

Fig. 6. XPS spectra of TiO_2 and TiO_2-GOx: (A) survey spectrum, (B) Ti 2p, (C) N 1 s, and (D) O 1S. (For interpretation of the references to colour in this figure legend, the reader is referred to the web version of this article).

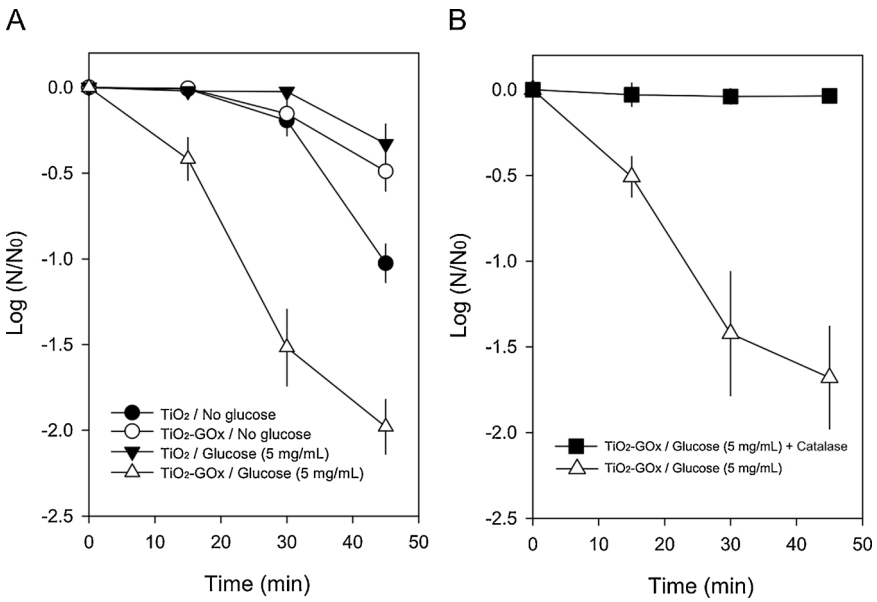

Fig. 8. (A) Antibacterial performance of TiO_2 and TiO_2-GOx with and without glucose. (B) Effect of catalase on antibacterial performance of TiO_2-GOx with glucose.

poor activity of pristine TiO_2 in the presence of glucose also implied bacterial resistance to ROS in the presence of abundant carbon sources in an aquatic environment. Interestingly, the antibacterial activity of TiO_2-GOx in the absence of glucose was inferior to that of native TiO_2 after 45 min. This may be due to the GOx layer reducing the ROS generation compared to pristine TiO_2. However, when glucose is present, the oxidation of glucose by glucose oxidase can compensate for the limited generation of ROS from the TiO_2-GOx by producing more H_2O_2.

We presumed that the H_2O_2 generated from the glucose oxidation by glucose oxidase on the surface of TiO_2 was a major ROS source that enhanced the antibacterial performance of TiO_2-GOx in the presence of glucose. To confirm this, we compared the antibacterial performance of TiO_2-GOx in the presence of both glucose and catalase under UV irradiation. Catalase is an enzyme that decomposes millions of molecules of H_2O_2 to water and oxygen per second, while protecting cells from oxidative damage caused by ROS [36,37]. The $\log(N/N_0)$ value of TiO_2-GOx without catalase in the presence of glucose after 45 min of UV exposure was -1.68, while that of TiO_2-GOx with catalase was -0.03, indicating that almost no bacteria were killed in the presence of catalase (Fig. 8(B)). We are certain that the catalase decomposes the H_2O_2 generated from glucose oxidation by glucose oxidase. The ROS generated as a result of photocatalytic activation by TiO_2-UV interaction were also believed to be decomposed, because hardly any inhibition of bacteria occurred when catalase was present in the sample, unlike the case in Fig. 8(A). Further, we measured the H_2O_2 concentration directly using the Amplex Red method when TiO_2-GOx or TiO_2 was used with glucose, without glucose, and with glucose/catalase. Fig. 9 shows that the H_2O_2 concentration generated by TiO_2 was similar in all the cases, while TiO_2-GOx generated large amounts of H_2O_2 in the presence of glucose. As expected from the results shown in Fig. 8(B), the presence of catalase diminished the H_2O_2 concentration. Based on all the results, we expect that the generation of large amounts of H_2O_2 from TiO_2-GOx in the presence of glucose was the key to enhancing the antibacterial performance of TiO_2-GOx.

We further conducted ESR analysis to investigate the difference in the type of ROS being generated from TiO_2 or TiO_2-GOx with glucose under UV irradiation. The ESR spin trapping of superoxide radical anions ($^{\cdot}O_2^-$), and hydroxyl radicals ($^{\cdot}OH$) with DMPO is widely used to investigate the production of superoxide and OH radicals in biological samples or TiO_2 [38–41]. Fig. 10 shows the ESR spectra of TiO_2 and TiO_2-GOx in the presence of glucose (5 mg/mL) and DMPO (10 mM) under UV irradiation. In the case of TiO_2, one spin adduct, the OH

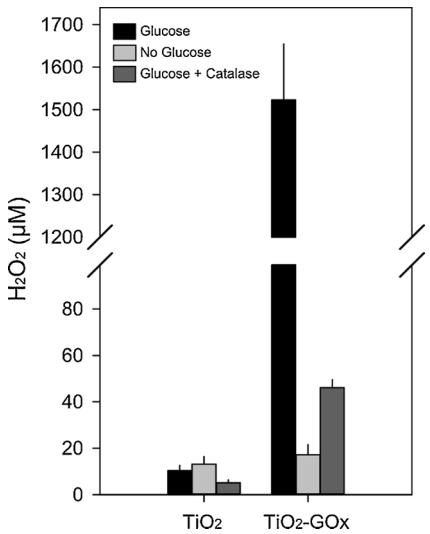

Fig. 9. Concentration of H_2O_2 produced by TiO_2 or TiO_2-GOx with glucose, no glucose, and glucose/catalase under UV irradiation.

radical (·OH), was predominantly generated (Fig. 10(A)). When TiO_2-GOx was exposed to glucose and UV, two spin adducts, superoxide (the peaks indicated by using red triangles) and the OH radical, were formed (Fig. 10(B)) [38]. The ESR spectrum of TiO_2 did not show the significant superoxide peaks observed for TiO_2-GOx. Without glucose, both TiO_2 and TiO_2-GOx showed predominantly OH radical peaks (data not shown). The production of H_2O_2 by GOx can be explained using ping-pong mechanisms such as those given in Eqs. (1) and (2) below:

$$E_{ox} + \text{glucose} \rightarrow E_{red} + \text{gluconic acid (gluconolactone)} \quad (1)$$

$$E_{red} + O_2 \rightarrow E_{ox} + H_2O_2 \quad (2)$$

where E_{ox} represents with FAD (flavin adenine dinucleotide), which is a common reactant in biological redox reactions, in the oxidized form, and E_{red} represents FAD in the reduced form [16]. The intermediate reaction of Eq. (2) involves the transformation of oxygen into superoxide; this superoxide is then transformed into H_2O_2 by the redox reaction involving GOx and the FAD complex. We surmised that the more intense superoxide peaks in the ESR spectrum of TiO_2-GOx were

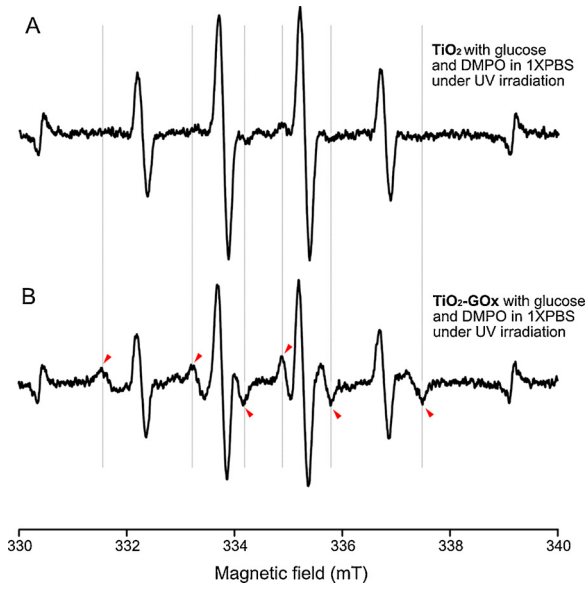

Fig. 10. ESR spectra of (A) TiO_2 and (B) TiO_2-GOx with glucose (5 mg/mL) and DMPO (10 mM) in 1 X PBS (pH 7.0) under UV irradiation (Red triangles indicate superoxide peaks) (For interpretation of the references to colour in this figure legend, the reader is referred to the web version of this article).

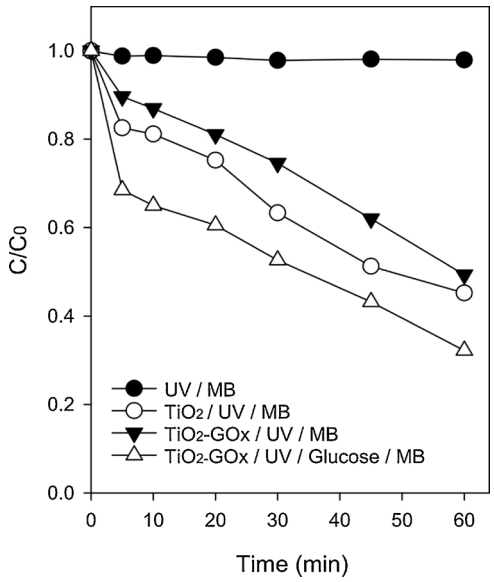

Fig. 12. Degradation of methylene blue under different catalytic conditions.

generated due to the enzymatic reaction of GOx with glucose rather than the interaction between TiO_2 and UV. Based on the direct measurement of H_2O_2 and the ESR analysis, TiO_2-GOx was found to produce more H_2O_2 and various ROS compared to TiO_2 in the presence of glucose and irradiation. As a result, the greater diversity of ROS species produced by TiO_2-GOx and glucose is thought to have improved the antibacterial performance.

Further, we investigated the antibacterial performance of TiO_2-GOx particles on *B. subtilis,* a gram-positive bacterium, and compared the results with those of *E. coli*, a gram-negative bacterium. Fig. 11 shows that TiO_2-GOx has a better antibacterial performance for both gram-negative (*E. coli*) and gram-positive (*B. subtilis*) bacteria compared to pristine TiO_2 particles in presence of glucose under UV irradiation. Although we only tested two types of bacteria in this study, the TiO_2-GOx particles could be used for inactivating other pathogenic bacteria in the presence of glucose with the UV-assisted disinfection process.

We also investigated how the presence of glucose affected the degradation of MB using TiO_2-GOx under UV irradiation. The degradation of MB using TiO_2 [42–44] or H_2O_2 [45,46] under UV irradiation has been extensively studied. To add to the existing literature, we investigated whether TiO_2-GOx could enhance the degradation of MB in the presence of glucose in aqueous environments. Fig. 12 shows that MB was not degraded when subjected to UV irradiation alone; however, it was degraded when combined with TiO_2 or TiO_2-GOx under UV irradiation. Almost 50% of the MB was degraded with TiO_2 after 60 min. Similar results were observed using TiO_2-GOx, although the speed of degradation was slower than that for TiO_2. When we mixed glucose with TiO_2-GOx under UV irradiation, 70% of MB was degraded after 60 min. This was the best performance among the other experimental

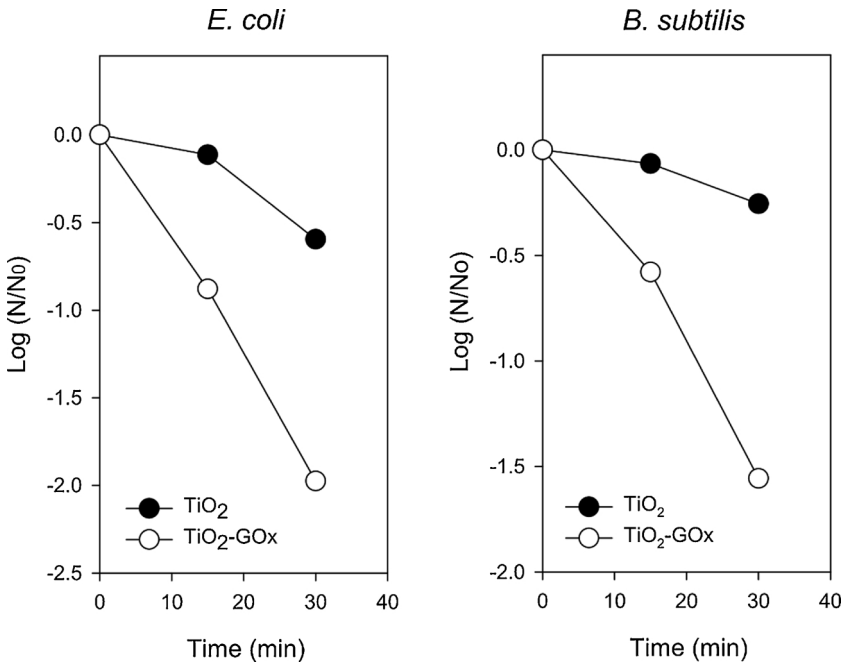

Fig. 11. Antibacterial performance of TiO_2 or TiO_2-GOx against *E. coli* (gram-negative bacterium) and *B. subtilis* (gram-positive bacterium).

conditions studied. We suspected that the additional H_2O_2 production might enhance the degradation of MB in the presence of glucose, as was the case for antibacterial performance.

4. Conclusion

We used TiO_2-GOx, inorganic–organic hybrid catalysts to enhance antibacterial performance in the presence of glucose and UV irradiation in aqueous environments. TiO_2-GOx has greater disinfecting ability than only TiO_2 alone under the above-mentioned conditions. In addition, TiO_2-GOx showed enhanced MB degradation compared to TiO_2 in the presence of both UV irradiation and glucose. We suspect that the synergetic production of H_2O_2 and superoxide, which was triggered by the oxidation of glucose by the glucose oxidase attached to the surface of the TiO_2 particles, can enhance the disinfection and degradation of the targets with OH radicals produced dominantly by the interaction of TiO_2 with UV. This phenomenon was investigated by measuring the H_2O_2 concentration, which allowed us to verify that H_2O_2 is the dominant species in the disinfection process as confirmed by the diminished amount of H_2O_2 in the presence of catalase and by measuring superoxide in the ESR analysis of TiO_2-GOx in the presence of glucose with UV irradiation. Considering the fact that wastewater is suspected to have a high glucose content as a carbon source for blooming microorganisms in an aqueous environment, inorganic–organic hybrid catalysts such as TiO_2-GOx will be useful for either efficient disinfection or the degradation of pollutants.

Acknowledgements

This work was financially supported by the KIST-UNIST partnership program (1.170086.01/2V05720), the Korean Ministry of Environment as part of “The Eco-Innovation Program” (No. 2016000140006), and the Korea Institute of Science and Technology (KIST) research programs (2E28160).

References

[1] C. Wei, W.Y. Lin, Z. Zainal, N.E. Williams, K. Zhu, A.P. Kruzic, R.L. Smith, K. Rajeshwar, Environ. Sci. Technol. 28 (1994) 934–938.
[2] S. Kim, K. Ghafoor, J. Lee, M. Feng, J. Hong, D.U. Lee, J. Park, Water Res. 47 (2013) 4403–4411.
[3] A.G. Rincon, C. Pulgarin, Appl. Catal. B-Environ. 44 (2003) 263–284.
[4] M. Okuda, T. Tsuruta, K. Katayama, Phys. Chem. Chem. Phys. 11 (2009) 2287–2292.
[5] M. Cho, H. Chung, W. Choi, J. Yoon, Water Res. 38 (2004) 1069–1077.
[6] J.C. Ireland, P. Klostermann, E.W. Rice, R.M. Clark, Appl. Environ. Microb. 59 (1993) 1668–1670.
[7] Y. Kikuchi, K. Sunada, T. Iyoda, K. Hashimoto, A. Fujishima, J. Photochem. Photobiol. A: Chem. 106 (1997) 51–56.
[8] J. Moan, K. Berg, Photochem. Photobiol. 53 (1991) 549–553.
[9] E. Linley, S.P. Denyer, G. McDonnell, C. Simons, J.Y. Maillard, J. Antimicrob. Chemother. 67 (2012) 1589–1596.
[10] F. Harber, J. Weiss, Proc. R. Soc. Lond. A Math. Phys. Sci. 147 (1934) 332–351.
[11] J.P. Kehrer, Toxicology 149 (2000) 43–50.
[12] L.A. Schaider, K.M. Rodgers, R.A. Rudel, Environ. Sci. Technol. 51 (2017) 7304–7317.
[13] W.C. Quayle, A. Fattore, R. Zandona, E.W. Christen, M. Arienzo, Water Sci. Technol. 60 (2009) 2521–2528.
[14] A. Bren, J.O. Park, B.D. Towbin, E. Dekel, J.D. Rabinowitz, U. Alon, Sci. Rep. 6 (2016) 24834.
[15] S.B. Bankar, M.V. Bule, R.S. Singhal, L. Ananthanarayan, Biotechnol. Adv. 27 (2009) 489–501.
[16] Q.J. Su, J.P. Klinman, Biochemistry 38 (1999) 8572–8581.
[17] M. Tiina, M. Sandholm, Int. J. Food Microbiol. 8 (1989) 165–174.
[18] D. Dobbenie, M. Uyttendaele, J. Debevere, J. Food Protect. 58 (1995) 273–279.
[19] S. Sagona, B. Turchi, F. Fratini, M. Giusti, B. Torracca, R. Nuvoloni, D. Cerri, A. Felicioli, B. Insectol. 68 (2015) 233–237.
[20] M.A. Zia, A. Riaz, S. Rasul, R.Z. Abbas, Braz. Arch. Biol. Technol. 56 (2013) 956–961.
[21] J. Vartiainen, M. Ratto, S. Paulussen, Packag. Technol. Sci. 18 (2005) 243–251.
[22] J.E. Ellingsen, Biomaterials 12 (1991) 593–596.
[23] Y. Kang, X. Li, Y.Q. Tu, Q. Wang, H. Agren, J. Phys. Chem. C 114 (2010) 14496–14502.
[24] S.T. Liu, X.Y. Meng, J.M. Perez-Aguilar, R.H. Zhou, Sci. Rep. 6 (2016) 37761.
[25] M. Horie, K. Nishio, K. Fujita, S. Endoh, A. Miyauchi, Y. Saito, H. Iwahashi, K. Yamamoto, H. Murayama, H. Nakano, N. Nanashima, E. Niki, Y. Yoshida, Chem. Res. Toxicol. 22 (2009) 543–553.
[26] B.C. Kim, I. Lee, S.J. Kwon, Y. Wee, K.Y. Kwon, C. Jeon, H.J. An, H.T. Jung, S. Ha, J.S. Dordick, J. Kim, Sci. Rep. 7 (2017) 40202.
[27] T.L. Chen, H.S. Weng, Biotechnol. Bioeng. 28 (1986) 107–109.
[28] J. Kong, S. Yu, M. Xu, Acta Biochim. Biophys. Sin. 39 (2007) 549–559.
[29] M.J. Baker, J. Trevisan, P. Bassan, R. Bhargava, H.J. Butler, K.M. Dorling, P.R. Fielden, S.W. Fogarty, N.J. Fullwood, K.A. Heys, C. Hughes, P. Lasch, P.L. Martin-Hirsch, B. Obinaju, G.D. Sockalingum, J. Sulé-Suso, R.J. Strong, M.J. Walsh, B.R. Wood, P. Gardner, F.L. Martin, Nat. Protoc. 9 (2014) 1771–1791.
[30] I. Otsuka, M. Yaoita, S. Nagashima, M. Higano, Electrochim. Acta 50 (2005) 4861–4867.
[31] K. Fujiwara, Y. Deligiannakis, C.G. Skoutelis, S.E. Pratsinis, Appl. Catal. B-Environ. 154 (2014) 9–15.
[32] Y. Kim, H.M. Hwang, L. Wang, I. Kim, Y. Yoon, H. Lee, Sci. Rep. 6 (2016) 25212.
[33] J.C. Tristao, F. Magalhaes, P. Corio, M.T.C. Sansiviero, J. Photochem. Photobiol. A 181 (2006) 152–157.
[34] G.J. Thomas, Annu. Rev. Biophys. Biomol. 28 (1999) 1–27.
[35] E. Vanea, V. Simon, Appl. Surf. Sci. 257 (2011) 2346–2352.
[36] H.N. Kirkman, G.F. Gaetani, Proc. Natl. Acad. Sci. U. S. A. 81 (1984) 4343–4347.
[37] P. Nicholls, I. Fita, P.C. Loewen, Adv. Inorg. Chem. 51 (2001) 51–106.
[38] X.Y. Feng, P.F. Wang, J. Hou, J. Qian, Y.H. Ao, C. Wang, J. Hazard. Mater. 351 (2018) 196–205.
[39] G.R. Buettner, Free Radic. Res. Com. 19 (1993) S79–S87.
[40] K. Ranguelova, R.P. Mason, Magn. Reson. Chem. 49 (2011) 152–158.
[41] D. Dvoranova, Z. Barbierikova, V. Brezova, Molecules 19 (2014) 17279–17304.
[42] R.S. Dariani, A. Esmaeili, A. Mortezaali, S. Dehghanpour, Optik 127 (2016) 7143–7154.
[43] C. Xu, G.P. Rangaiah, X.S. Zhao, Ind. Eng. Chem. Res. 53 (2014) 14641–14649.
[44] R.F. Zuo, G.X. Du, W.W. Zhang, L.H. Liu, Y.M. Liu, L.F. Mei, Z.H. Li, Adv. Mater. Sci. Eng. (2014) 170148.
[45] L.V. Jian-xiao, Y. Cui, G.H. Xie, L.Y. Zhou, S.F. Wang, J. Water Reuse Desalin. 1 (2011) 45–51.
[46] J. Jiang, J. Zou, L. Zhu, L. Huang, H. Jiang, Y. Zhang, J. Nanosci. Nanotechnol. 11 (2011) 4793–4799.